Soliton as Strange Attractor: Nonlinear Synchronization and Chaos

J. M. Soto-Crespo[1] and Nail Akhmediev[2]
[1]Instituto de Óptica, C.S.I.C., Serrano 121, 28006 Madrid, Spain
[2]Optical Sciences Group, Research School of Physical Sciences and Engineering, The Australian National University, Canberra ACT 0200, Australia
(Received 7 March 2005; published 8 July 2005)

We show that dissipative solitons can have dynamics similar to that of a strange attractor in low-dimensional systems. Using a model of a passively mode-locked fiber laser as an example, we show that soliton pulsations with periods equal to several round-trips of the cavity can be chaotic, even though they are synchronized with the round-trip time. The chaotic part of this motion is quantified using a two-dimensional map and estimating the Lyapunov exponent. We found a specific route to chaotic motion that occurs through the creation, increase, and overlap of ''islands'' of chaos rather than through multiplication of frequencies.

DOI: 10.1103/PhysRevLett.95.024101 PACS numbers: 05.45.Yv, 05.45.Xt, 42.55.Wd

Solitons are usually considered to be stable self-localized objects that do not show any chaotic behavior. This is true for solitons in integrable systems, but is certainly not the case for solitons in dissipative systems. Dissipative solitons exist in various physical arrangements [1] including binary liquids, all-optical transmission lines, and chemical reactions. As an example of an optical system generating chaotic dissipative solitons, we consider a laser with passive mode locking.

Passively mode-locked lasers producing ultrashort pulses can operate in a regime of period multiplication [2–6]. This occurs when the pulse does not recover its shape after traveling exactly one round-trip, but it can do so after several round-trips. Solitons can acquire additional pulsations with a period that differs from the round-trip time. In particular, period 2 pulsations have been observed in a solid state laser [3]. Periods 2, 3, and 6 have been observed in a nonlinear fiber ring resonator [7]. Much longer periods of pulsations (up to a few hundred round-trips) have been observed in a passively mode-locked fiber laser [8]. When the period of the pulsations is just a few round-trips of the cavity, it can easily be synchronized with the round-trip time, although elements of chaotic behavior may be present [9]. On the other hand, when the period of pulsations is much longer than the round-trip time, these chaotic behaviors can dominate.

This synchronization occurs for parameters of the system located in small windows of the parameter space. There are several of these windows with synchronization number N (the number of round-trips in the additional period of the pulsations), varying from 2 (period-doubling) to hundreds and thousands of round-trips. Beyond those windows, we can find chaotic behavior of the solitons. Our main interest in this work is the soliton dynamics at the edges of these windows, i.e., the transition from synchronization to chaotic behavior. In particular, we show that the synchronization of the pulsation period with the round-trip time can occur but it can also be supplemented with chaotic dynamics. The chaotic part of the dynamics forces the soliton to behave like a strange attractor in low- dimensional systems. The conjecture that a dissipative soliton can behave as a strange attractor was proposed in Ref. [10]. In the present work, we confirm this conjecture quantitatively using the laser model analyzed in Ref. [8].

We model a fiber laser using the cubic-quintic complex Ginzburg-Landau equation (CGLE) [11] with parameter management:

$$i\psi_z + \frac{D}{2}\psi_{tt} + |\psi|^2\psi + \nu|\psi|^4\psi = i\delta\psi + i\epsilon|\psi|^2\psi + i\beta\psi_{tt} + i\mu|\psi|^4\psi, \quad (1)$$

where z is the distance that the pulse travels in the cavity, t is the retarded time, ψ is the normalized envelope of the field, D is the group velocity dispersion coefficient, δ is the linear gain-loss coefficient, $i\beta\psi_{tt}$ accounts for spectral filtering ($\beta > 0$), $\epsilon|\psi|^2\psi$ represents the nonlinear gain which arises from saturable absorption, the term with μ represents, if negative, the saturation of the nonlinear gain, while the one with ν corresponds, also if negative, to the saturation of the nonlinear refractive index.

The laser cavity consists of several pieces of fiber, connecting the different elements and the mode-locking device. The properties of the media where the pulse propagates vary with the distance. Hence, the coefficients in Eq. (1) must be periodic functions of the distance z. We take the coefficients in the equation (1) to be periodic stepwise functions of z. Each period naturally describes one round-trip of the optical pulse. The model is illustrated in the inset of Fig. 1. It is the same as in Ref. [8]. The section of the erbium-doped fiber, together with the passive mode-locking element, is modeled by the full CGLE equation, where all the equation parameters generally differ from zero (see the left-hand-side box of this figure). The dispersion in this section of the cavity is taken to be normal ($D < 0$) and the length of the section is L_D. The single-

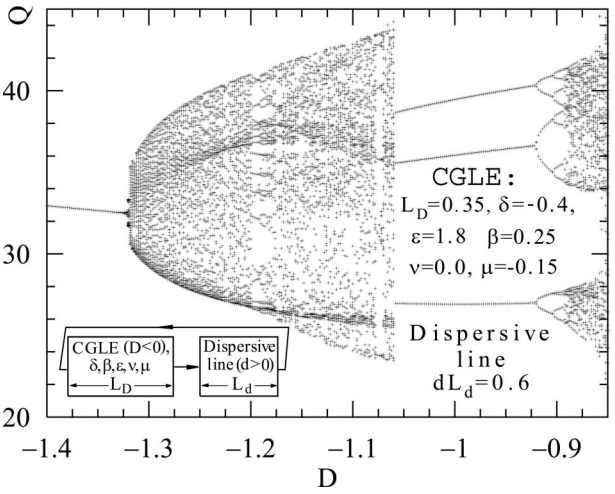

FIG. 1. Bifurcation diagram showing the period-tripling bifurcation with an additional long-period pulsation. The inset shows the laser model used in the numerical simulations.

mode fiber with anomalous dispersion ($D = d > 0$) is modeled by the same equation with only the dispersive term taken into account (the right-hand-side box of this figure). The length of this fiber is denoted by L_d. The equation in this part is linear, and therefore the only relevant parameter is the product (dL_d). The Kerr nonlinearity of the fiber is assumed to be negligible in comparison with the nonlinear response of the ''mode locker'' in the system. The pulse profile is monitored once every round-trip at the end of this section. As output data, we use the soliton amplitude A and calculate the pulse energy $Q = \int |\psi|^2 dt$. These are functions of the system parameters, and they usually take the form of bifurcations rather than smooth curves. When the pulse profile changes from one round-trip to another, these functions additionally become multivalued.

Figure 1 shows an example of a bifurcation diagram taken from Ref. [8]. The figure represents the obtained output values of the pulse energy, Q, as a function of the dispersion parameter D, after any transitory behavior has been removed. It shows the transition from a single period to a period 3 solution. Specifically, the period one can be seen clearly in the region below $D \approx -1.32$. The period 3 solution exists in the interval $-1.05 < D < -0.92$. In between these two regimes, we can see a wide area of soliton evolution with a continuous range of allowed values for Q. This area corresponds to the quasiperiodic soliton evolution with an additional period involved in its dynamics. This additional period is not exactly a multiple of the round-trip time, thus creating in Fig. 1 the region with a continuous interval of energies. The period changes from N being infinite at $D = -1.32$ to $N = 3$ at $D = -1.06$. The amplitude of the long-period modulation changes from zero on the left-hand side to its maximum value on the right-hand side of this interval.

When an additional period appears, it is, generally, incommensurate with the round-trip time. However, for some range of parameters, the ''synchronization'' (or entrainment) of two frequencies can occur. Then, a period which is an integer multiple of the round-trip time can be observed. A clear example of such synchronization is the period 3 solution in the interval $-1.06 < D < -0.92$. Another example can be seen in Fig. 1 in a small window in the region $-1.2 < D < -1.19$. The soliton energy takes discrete values rather than arbitrary values from the continuous range. This can be seen clearly if we plot the same figure with a higher resolution in D (see Fig. 2). The solution for D around -1.195 has 19 fixed values of energy. Three other zones with discrete values of the energy can be seen in this figure for D equal to ≈ -1.175, ≈ -1.152, and ≈ -1.128, with periods 16, 13, and 10 round-trips, respectively. These three windows have similar structures with chaotic motion at their boundaries.

The question arises whether the motion in these regions is a regular two-period oscillation of the soliton parameters or chaotic dynamics. The presence of the sequence of period-doubling bifurcations for D below approximately -1.191 indicates that the motion may be chaotic, at least just above this point. At the same time there could be elements of synchronization and chaos simultaneously. In order to find out, we studied the soliton dynamics on the right-hand side of the window with period equal to ten round-trips, namely, at $D = -1.127$. In contrast to what happens on the left-hand side part of this window, the motion here is not an exact period ten solution. A given value of the soliton energy Q does not return to the same value after ten round-trips. It slightly changes each time, creating a small band of admissible values. The size of these bands increases from being a point (which corresponds to a fixed point of the dynamical system) on the left-hand-side part of the window to a finite-size band on the right-hand-side part. These bands are nothing else but

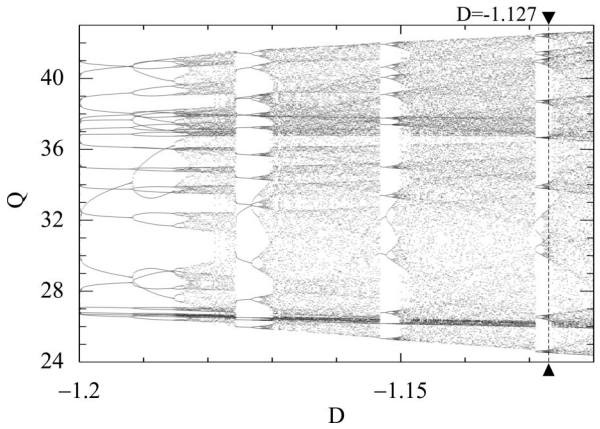

FIG. 2. Part of the bifurcation diagram in Fig. 1 that shows synchronization (entrainment) and transition to chaos.

islands of chaotic motion. As a result, we still have the period ten solution, but with some amount of chaotic dynamics. Synchronization occurs, but it is accompanied by a chaotic component of the motion.

Thus, at the value $D = -1.127$, the pulse enters a regime of ''chaotic resonance.'' We have now a period ten motion but the pulse parameters ''jitter.'' Instead of fixed values, we have a band for each tenth round-trip. In order to show that these bands are islands of chaos within the regular synchronized motion, we constructed a one-dimensional Poincaré map of this motion. Figure 3 shows the energy Q of the pulse after ten round-trips as a function of Q before them. The ten bands of values of Q, corresponding to every tenth round-trip, are clearly seen. Two pairs of bands [labeled (6, 7) and (5, 9)] in the intervals $29.5 < Q < 33$ and $40 < Q < 42$ overlap in energy, but they are distinctively different on the map.

All bands are located close to the diagonal line of the plot. This occurs due to the fact that each tenth iteration returns the point to the same band. The numbers next to the curves indicate the relative order in which the nearest iterations follow each other. The plot reveals a certain structure of these bands resembling ten separate horseshoe curves. A magnified image of one of the bands (the one labeled 3 in Fig. 3) is shown in the inset of this figure. All the other bands have similar structures. We can see this by comparing the curve in the inset with the largest bands 6 and 7 in Fig. 3. At first glance, each band could be interpreted as a noninvertible (logistic-type) map. This map is known to result in chaotic motion [12]. If we approximate the curve in the inset in Fig. 3 with a single parabola it will give chaotic motion. In reality, the map has a more complicated structure than just an inverted parabolic shape.

The curve in the inset in Fig. 3 has two branches of almost parabolic shape located very close to each other. Each successive iteration of this map may appear on either of the two branches, independently of where it started. Transitions between the two branches are unpredictable, showing that the approximation by a one-dimensional map is inadequate for a description of the motion. Therefore, we are faced with the necessity of constructing at least a two-dimensional map. To construct such a map, we choose the soliton amplitude A as the second variable. Similar results are obtained for any other soliton parameter that can be calculated uniquely.

Figure 4 shows the two-dimensional map of the variables (Q, A) calculated for the same band 3. The two insets show successive magnifications of small parts of the map that allow us to resolve the fine details of the curves. The lines have a fractal structure similar to that obtained for the Hénon map [12]. This is one of the features of the chaotic behavior of the trajectories inside a strange attractor. We can conclude that solitons in our model behave as strange attractors at some values of the parameters. We conjectured this in our earlier work [10], and now we show that the conjecture was true.

In order to further show that the motion is chaotic, we have to show that any two initially-nearby trajectories diverge in the phase space. This can be done if we choose some parameter of the motion that approximates the separation between the trajectories in an infinite-dimensional phase space and show that it increases. As such parameter, we can take the separation between two nearby points on the two-dimensional map in Fig. 4. Namely, we define the separation according to the formula

$$S_{I,J} = \sqrt{(Q_I - Q_J)^2 + (A_I - A_J)^2}, \qquad (2)$$

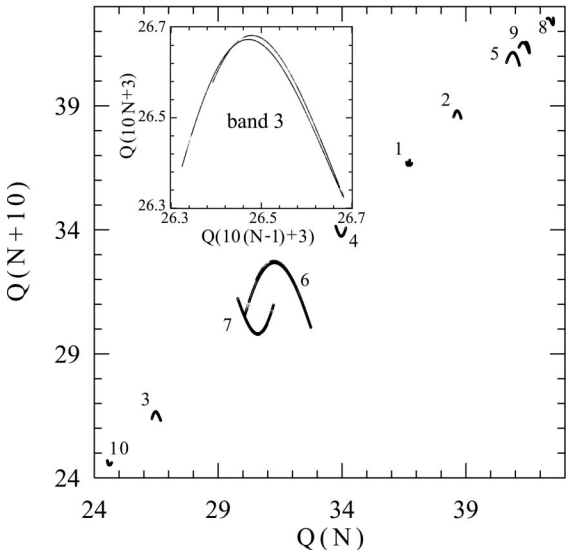

FIG. 3. One-dimensional map for partially synchronized period 10 pulsations. The inset presents a magnified image of the third band. It shows the fine structure of the band which has a shape of a double horseshoe. Other bands have similar substructure.

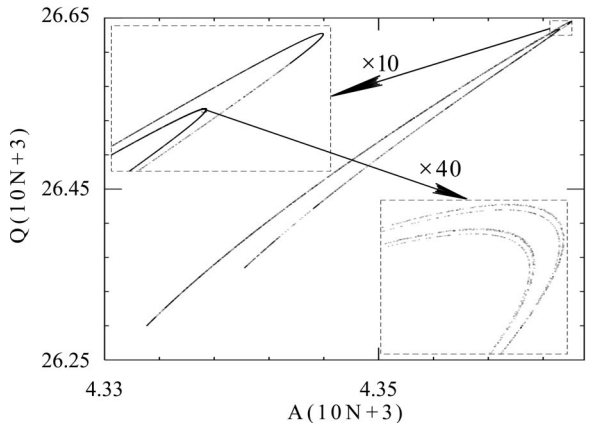

FIG. 4. Two-dimensional (soliton energy Q vs soliton amplitude A) map of period-10 pulsations. Two consecutive magnifications, indicated by arrows, show the fractal structure of the map. The magnification factor is written on the arrows.

where indices I and J attribute the parameters to two different points of the map.

The separation will change during the evolution, and it depends on the number of round-trips n made by the pulse in the cavity, so $S_{I,J} = S_{I,J}(n)$. Let us suppose that this separation changes exponentially with n:

$$S_{I,J}(n) = S_{I,J}(0)\exp(10LN), \tag{3}$$

where $S_{I,J}(0)$ is the initial separation, $S_{I,J}(n)$ is the separation after $n = 10N$ round-trips, and L is the Lyapunov exponent. The factor 10 in the exponential function appears because we consider data after every ten round-trips. The initial separation, $S_{I,J}(0)$, has to be chosen small enough in order for the approximation (3) to be valid.

The motion can be considered chaotic when the Lyapunov exponent is positive. If we know the initial separation, $S_{I,J}(0)$, and the separation after ten round-trips, the Lyapunov exponent can be calculated as ($N = 1$)

$$L = \frac{1}{10}\log\left[\frac{S_{I,J}(10)}{S_{I,J}(0)}\right]. \tag{4}$$

For the pairs of points (I, J) in Fig. 4 that satisfy the condition $S_{I,J}(0) < 5 \times 10^{-8}$, we calculate the separation $S_{I,J}(10)$ and apply Eq. (4) to find the Lyapunov exponent. The results of the calculation of L for 15000 different pairs of points inside the band in Fig. 4 are shown in Fig. 5. The scattering of data in Fig. 5 is related to the fact that we have replaced the real separation in an infinite-dimensional phase space by the two-dimensional approximation (2). The average value of L calculated from these data is positive and equals to 0.13, which shows that the motion is indeed chaotic. The clearly visible dense stripes in Fig. 5 appear due to the fractal structure of the bands.

A further increase of D above -1.267 results in completely chaotic behavior. The sizes of the islands of chaos increase until they merge. Consecutive iterations no longer bring the point in Fig. 3 back to the same band after a fixed number of round-trips. The elements of synchronization disappear. Strange attractors of smaller size merge into a larger one. This is an example of a route to chaos which is different from the classic period-doubling sequence of bifurcations. The fixed points of purely periodic motion are first transformed into small islands of chaotic motion. The size of these islands increases until they all merge. The global chaotic solution appears as a result of the overlap between these islands of partially chaotic motion, rather than being due to a multiplication of frequencies. The choice of D as a variable in our simulations does not limit its generality. Similar transition into chaotic regime can be observed when we move in other directions in the multidimensional space of the system parameters in the vicinity of the same point.

In conclusion, we revealed chaotic dynamics of solitons in dissipative systems. We have shown that solitons generated by passively mode-locked lasers can contain elements of chaotic dynamics similar to that of a strange attractor in low-dimensional systems.

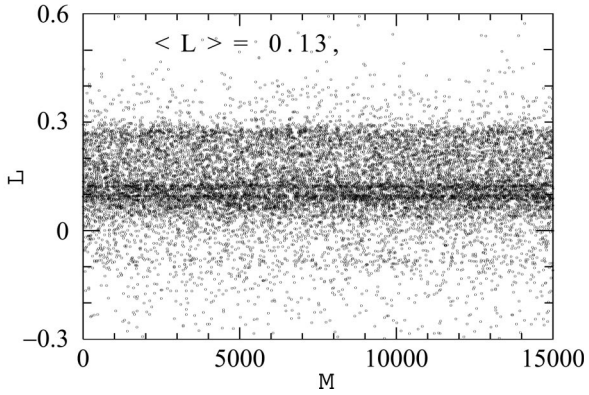

FIG. 5. Lyapunov exponents L calculated for 15000 pairs of points in the two-dimensional map (A, Q) using Eq. (4).

The work of J. M. S. C. was supported by the MCyT under Contract No. BFM2003-00427 and by the CAM under Contract No. GR/MAT/0425/2004. N. A. acknowledges support from the Australian Research Council. The authors are grateful to Dr. Ankiewicz for a critical reading of the manuscript.

[1] *Dissipative Solitons*, edited by N. Akhmediev and A. Ankiewicz (Springer, New York, 2005).
[2] K. Tamura, C. R. Doerr, H. A. Haus, and E. P. Ippen, IEEE Photonics Technol. Lett. **6**, 697 (1994).
[3] D. Côté and H. M. van Driel, Opt. Lett. **23**, 715 (1998).
[4] F. Ilday, J. Buckley, and F. Wise, *Proceedings of the Nonlinear Guided Waves Conference, Toronto, March 28–31, 2004* (OSA, Washington, DC, 2004), Paper MD9.
[5] Liguo Luo, T. J. Tee, and P. L. Chu, J. Opt. Soc. Am. B **15**, 972 (1998).
[6] G. Sucha, D. S. Chemla, and S. R. Bolton, J. Opt. Soc. Am. B **15**, 2847 (1998).
[7] S. Coen, M. Haelterman, Ph. Emplit, L. Delage, L. M. Simohamed, and F. Reynaud, J. Opt. Soc. Am. B **15**, 2283 (1998).
[8] J. M. Soto-Crespo, M. Grapinet, Ph. Grelu, and N. Akhmediev, Phys. Rev. E **70**, 066612 (2004).
[9] S. R. Bolton and M. R. Acton, Phys. Rev. A **62**, 063803 (2000).
[10] N. Akhmediev, J. M. Soto-Crespo, and A. Ankiewicz, in *Nonlinear Waves: Classical and Quantum Aspects*, edited by F. Kh. Abdullaev and V. V. Konotop (Kluwer, Dordrecht, 2004), pp. 45–60.
[11] H. A. Haus, J. Appl. Phys. **46**, 3049 (1975).
[12] E. Infeld and George Rowlands, *Nonlinear Waves, Solitons and Chaos* (Cambridge University Press, Cambridge, England, 2000), 2nd ed..